Supporting information

Efficient upcycling electroplating sludge and waste PET into Ni-MOF nanocrystals for effective photoreduction of CO_2

Kainan Song, [a] Xiaoqing Qiu, [d] Bin Han, [a] Shujie Liang, [a] Zhang Lin, *[abc]

[a] School of Environment and Energy, Guangdong Provincial Key Laboratory of Solid Wastes Polltion Control and Recycling, South China University of Technology, Guanghzou, 510006 (P. R. China). E-mail: zlin@scut.edu.cn

[b] School of Metallurgy and Environment, Central South University, Changsha, 410083 (P. R. China). E-mail: zhang_lin@csu.edu.cn

[c] Chinese National Engineering Research Center for Control & Treatment of Heavy Metal Pollution, 410083 Changsha, Hunan, China

[d] College of Chemistry and Chemical Engineering, Central South University, Changsha, 410083 (P. R. China)

Experimental Section

Chemicals and materials. $NiCl_2•6H_2O$, HCl, NaOH and absolute ethyl alcohol were bought from Sinopharm. Terephthalic acid (BDC, 99.0%), acetonitrile (MeCN) and triethanolamine (TEOA) were purchased from Aladdin. N, N-dimethylformamide (DMF) and $[Ru(bpy)_3]Cl_2•6H_2O$ were obtained from Macklin. All reagents were used as purchased with no further purification. Clear mineral water bottles (PET plastics) collected from domestic waste were used as the raw material. The electroplating sludge (EPS) was obtained from a factory in Guangdong province, China. Deionized water was used for all of the experiments in this work.

Acid leaching of the EPS. the raw sludge was first dried overnight to constant weights at 105 ^oC and then grinded to 100 mesh before further utilization. Typically, 5.0 g of the dried sludge was placed in a conical flask, followed by the addition of 25 mL of a hydrochloric acid solution (2.0 mol/L), magnetic stirring for 3 h, and then centrifuged (8000 rpm, 5 min). The supernatant was collected and filtered for further process. A larger volume or higher concentration of the HCl would be used for the completely leaching of Ni element from the sludge. The acid leaching solution was labeled as $Ni_{(aq)}$.

Alkaline hydrolysis of the PET plastic waste. The labels and caps of the clear mineral

water bottles were removed and then the bottles were cut into small pieces. The small flakes were washing with water and soap, and then dried in an oven overnight at 60 ^{o}C. PET hydrolysis experiment was carried out in a 100 mL Teflon-lined stainless steel autoclave and the product was labeled as BDC. 3.0 g of PET flakes were put into the autoclave with 1.248 g NaOH (2 equivalents with respect to BDC present in the PET) and 30 mL H_2O, then the autoclave was heated up to 200 ^{o}C and maintained for 6 h. After natural cooling, NaOH (2M) was introduced into the above mixture until pH 13 was reached, so that non-hydrolyzed PET (if any) could be removed by centrifugation. Next, the supernatant was acidified with 6M HCl to pH 1 and the white precipitated BDC was separated by centrifugation. After that, the BDC was washed twice with water and ethanol respectively, and vacuum-dried at 90 ^{o}C for 12 h.

Synthesis of Ni MOFs. The Ni MOFs was prepared via a solvothermal process according to previous work with minor modification. Firstly, 64 mL DMF, 4 mL ethanol and X mL ($X = 4 - V_{Ni(aq)}$) H_2O were mixed in a beaker. Secondly, 1.5 mmol BDC was added into the above mixture under magnetic stirring. Thirdly, 1.5 mmol $NiCl_2$•$6H_2O$ or a certain volume of $Ni_{(aq)}$ was added and kept stirring until Ni^{2+} completely dissolved. Then the above solution was transferred into a 100 mL Teflon-lined stainless steel autoclave and heated at 140 ^{o}C for 24 h. Finally, the products were obtained via centrifugation, washed with water and ethanol for 5 times, and dried using vacuum freeze dryer.

Synthesis of bulk $Ni(OH)_2$. 6 mmol $NiCl_2$•$6H_2O$ was dissolved in 54 mL H_2O under magnetic stirring, then 6 mL NaOH solution (2M) was added at 0.5 mL/min using a syringe pump. Then the above mixture was transferred into a 100 mL Teflon-lined stainless steel autoclave and heated at 180 ^{o}C for 12 h. Subsequently, the bulk $Ni(OH)_2$ was collected via centrifugation, washed with water and ethanol for 3 times, and dried by vacuum freeze-drying.

Photocatalytic CO_2 reduction. Typically, 1 mg of photocatalyst, 7.5 mg of $[Ru(bpy)_3]Cl_2$•$6H_2O$ (labeled as Ru, bpy = 2'2-bipyridine), 1 mL TEOA, 2 mL H_2O

and 3 mL MeCN were added into a gas-closed quartz bottle (~ 60 mL in capacity), respectively. The reaction devices were thoroughly degassed, and then backfilled with high purity CO_2. Subsequently, the quartz reactors were put in a multi-channel photocatalytic reaction system (PCX50A Discover, Beijing Perfect Light Technology Co., Ltd.) with several 5W white LED lights (400 nm - 1000 nm). During the photocatalytic reaction, the Ni MOF was continuously dispersed in the solution by a magnetic stirrer. After each irradiation time, 0.8 mL of product gases in the headspace of the reactor was withdraw through an Agilent gas-tight syringe and analyzed by an Agilent 7890B GC. The identities of product gases were determined by retention time and the yield of CO and H_2 were calculated by external standard method (Figure S10). Every sample was tested double times (the deviation was less than 3%) and got the average activity for photoreduction of CO_2. To evaluate photocatalyst reusability, 50 mg of the Ni MOF was used for photocatalytic reaction and recycled via a centrifuging, washing and drying process after each irradiation time, and then mixed with 7.5 mg of Ru, 1 mL TEOA, 2 mL H_2O and 3 mL MeCN for the next cycle.

The selectivity for CO was calculated using the equation below

$$\text{Selectivity of CO} = n(CO)/[n(CO) + n(H_2)] \times 100\%$$

The apparent quantum yield (AQY) was measured under the same photocatalytic reaction condition irradiated by a LED light (420 nm). The number of incident photons was measured using a radiant power energy meter (Ushio spectroradiometer, USR-40). The AQY was calculated according to the equation below:

$$\text{AQY}(\%) = \text{number of reacted electrons/number of incident electrons} \times 100\%$$

$$= \text{number of evolved } (CO + H_2) \text{ molecules} \times 2/\text{number of incident electrons} \times 100\%$$

Materials characterization. The crystal structure of the materials was analyzed on a Bruker D8 ADVANCE X-ray diffractometer equipped with Cu-Kα radiation. Field emission scanning electron microscopy (FE-SEM, Hitachi Regulus 8100) images, field emission transmission electron microscopy (FE-TEM, FEI Talos F200X) images and EDX elemental mapping images were collected for the characterization of structure and elemental distribution. X-ray photoelectron spectroscopy (XPS) measurements were

performed on a Thermo Scientific ESCA Lab250 spectrometer, and all of the binding energies were calibrated with respect to the C 1s peak at 284.6 eV. The N_2 adsorption/desorption isotherms on the adsorbent at 77K and CO_2 adsorption isotherm on the adsorbent at 298K were measured with a Micromeritics ASAP 2020 analyzer. Prior to gas adsorption measurements, all of the samples were degassed at 393K for 6 h. Electrochemical impedance spectroscopy (EIS) measurements were tested on an electrochemical workstation (CHI 660E) based on typical three-electrode system comprised of the Ni-MOF modified FTO glass as the current collector, platinum wire as the counter electrode, and saturated calomel electrode as the reference electrode. The EIS was recorded in a 0.1 M Na_2SO_4 solution with a frequency range from 0.01 Hz to 1MHz at 0.61V, and the amplitude of the applied sine wave potential in each case was 5 mV. Photoluminescence (PL) spectra and time-resolved PL spectra of the photocatalysts were collected on a FLS980 spectrometer under 540 nm laser irradiation at room temperature. The results were obtained in a TEOA/H_2O/MeCN (1 mL/2 mL/3 mL) mixture containing Ru (7.5 mg), which was as same as the photocatalytic CO_2 reduction reaction. The concentrations of metal ions in the acid leaching of the Ni sludge were analyzed by an inductively coupled plasma optic emission spectrometer (ICP-OES, Perkin Elmer Avio 200).

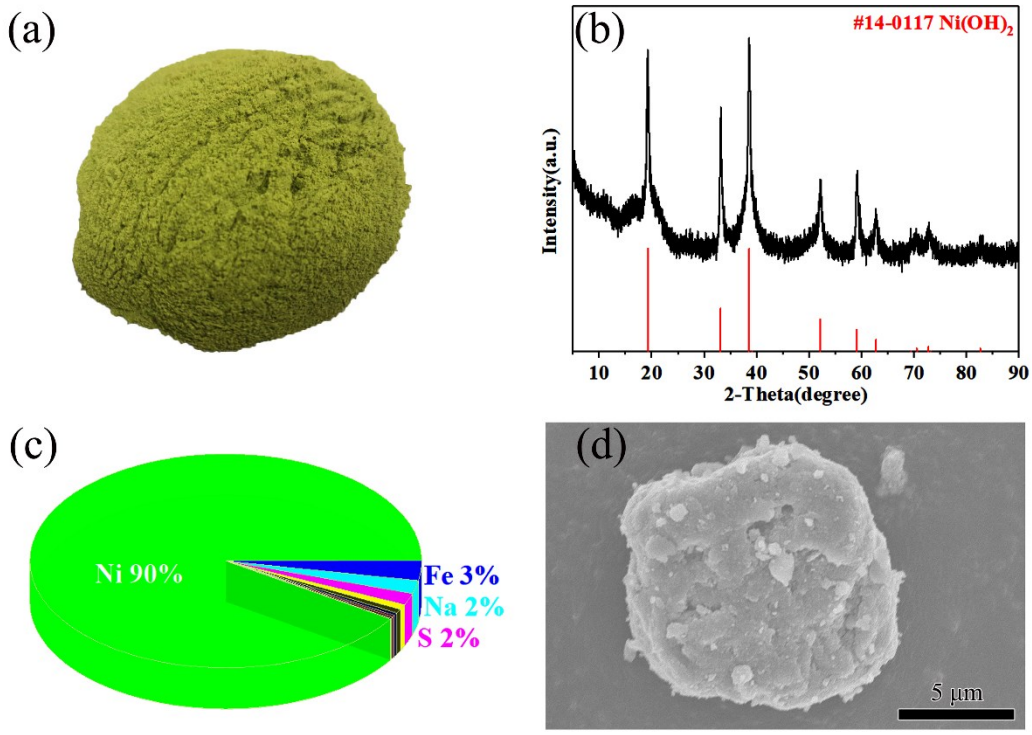

Figure S1. (a) Photograph of the Ni sludge, (b) XRD profile of the Ni sludge, (C) pie chart of the elemental composition of the Ni sludge determined by the XRF analysis, and (d) SEM image of pristine Ni sludge.

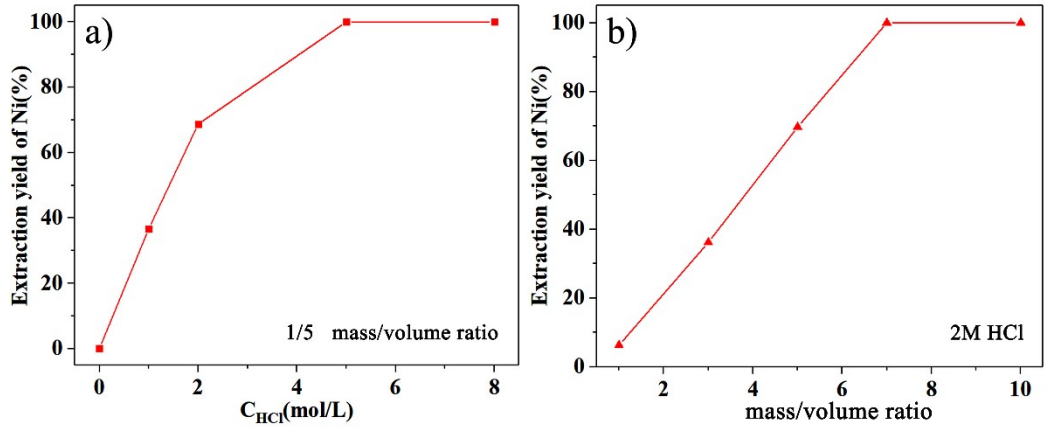

Figure S2. The effect of concentration a) and dosage b) of the HCl solution on the extraction yield of the Ni element.

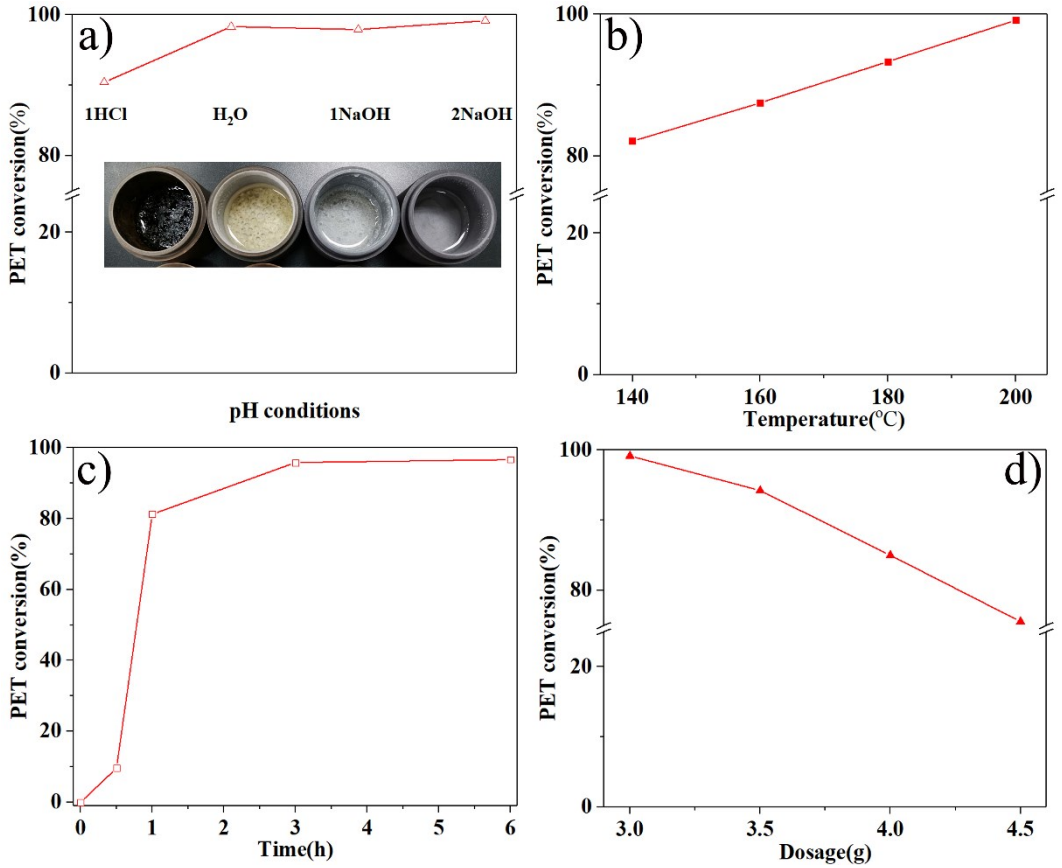

Figure S3. The effects of pH conditions a), temperature b), time c) and dosage of precursors d) on the conversion rate of PET flakes.

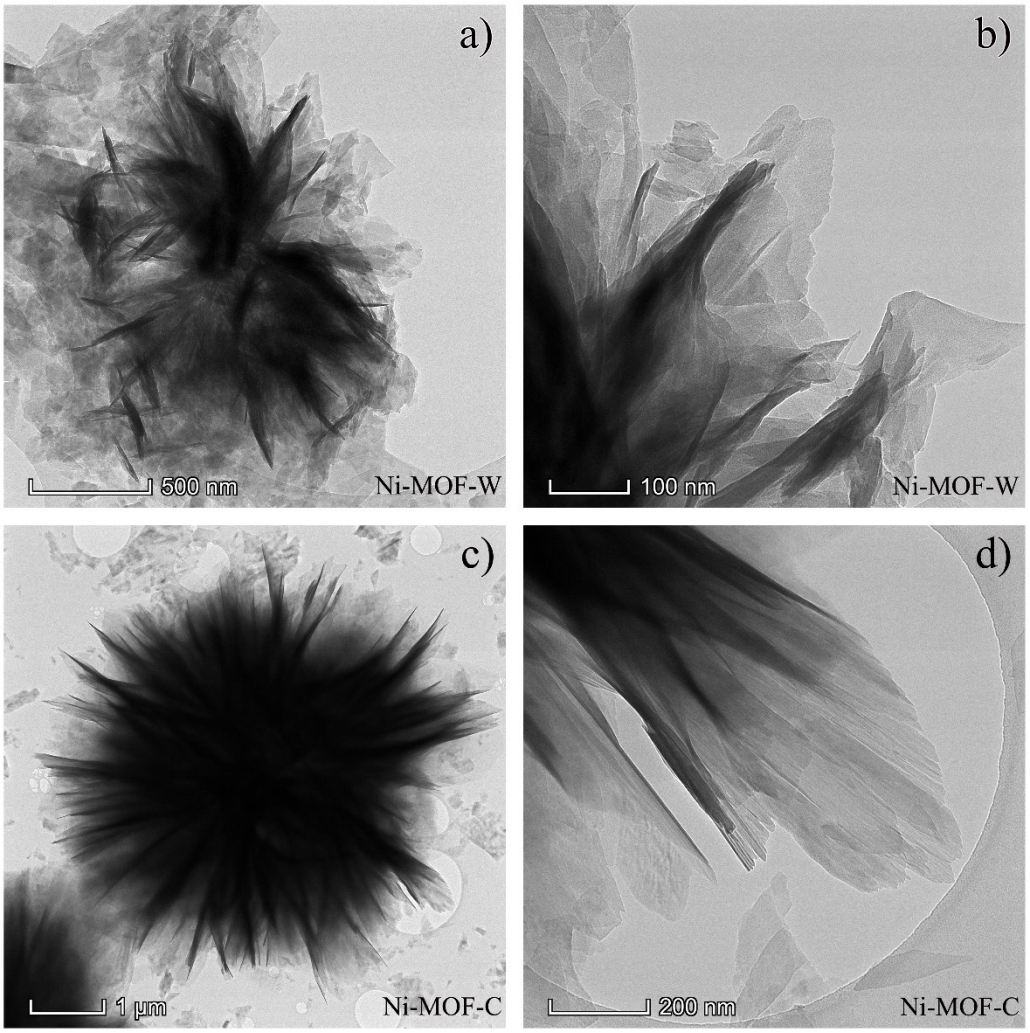

Figure S4. TEM images of the Ni-MOF-W (a and b) and Ni-MOF-C (c and d).

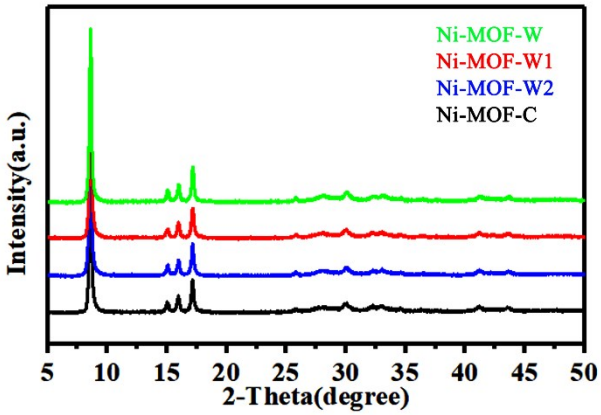

Figure S5. XRD patterns of the Ni-MOF synthesized from waste metal source (Ni-MOF-W2) or from waste PET plastic source (Ni-MOF-W1).

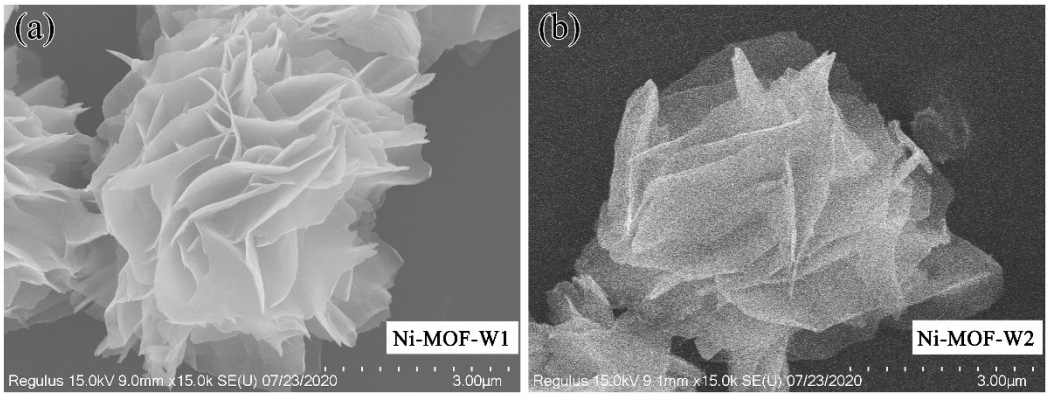

Figure S6. SEM images of the Ni-MOF synthesized from waste PET plastic source (Ni-MOF-W1) or from waste metal source (Ni-MOF-W2).

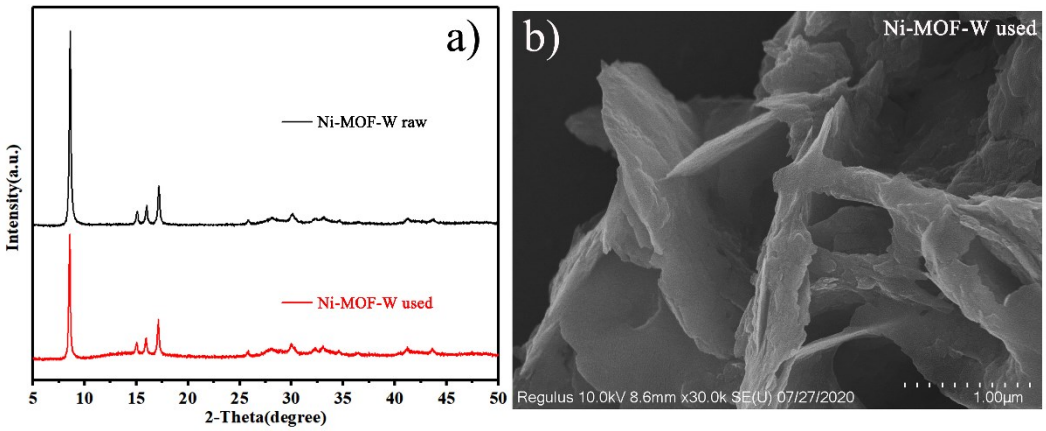

Figure S7. The XRD pattern a) and SEM image b) of the used Ni-MOF-W after the stability tests.

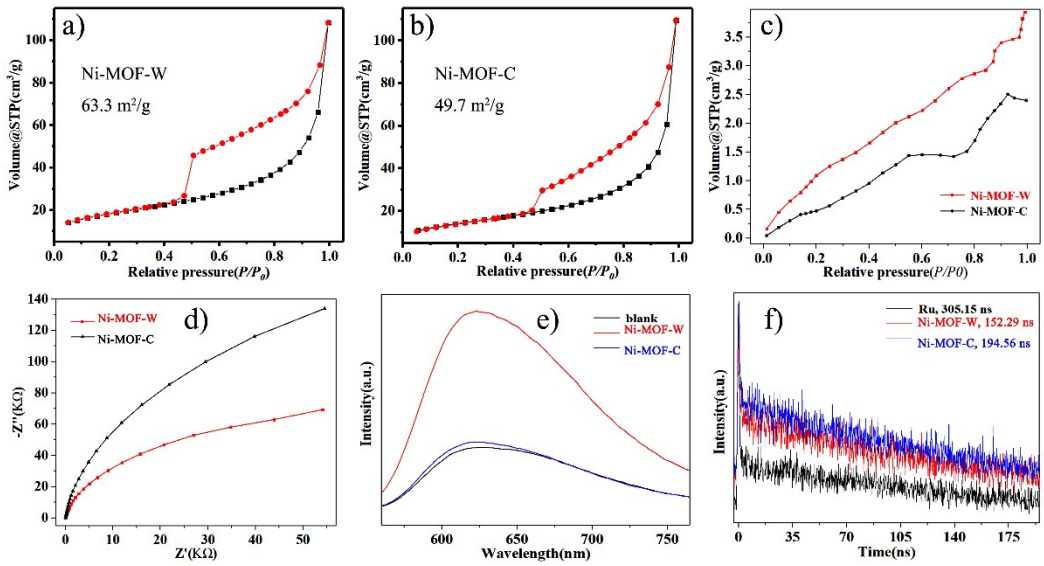

Figure S8. N_2 adsorption isotherms (a and b), CO_2 adsorption isotherms c), EIS spectra d), steady-state PL spectra e) and time-resolved transient PL decay spectra f) of the Ni-MOF-W and Ni-MOF-C.

In order to understand the high CO_2 reduction activity of the Ni-MOF-W, physical and photoelectrochemical characterizations have been carried out. The Ni-MOF-W exhibits a higher CO_2 uptake, a lower charge-transfer resistance and a shorter emission lifetime than that of the Ni-MOF-C (Figure S8). However, the steady-state PL intensity of the Ni-MOF-W is much stronger than that of the Ni-MOF-C, indicating an inefficient charge-carrier separation in Ni-MOF-W. All of these factors combine to create no better performance of the Ni-MOF-W than that of the Ni-MOF-C.

Table S1. The concentrations of metal ions in the acid leaching solution of the Ni-containing electroplating sludge

Samp./Conc.	Ni, mg/L	Na, mg/L	Fe, mg/L	Cu, mg/L	Al, mg/L	Zn, mg/L
1#	26.82	0.65	——	——	0.0001	——
2#	46.83	0.47	0.0019	0.032	——	——
3#	43.85	——	1.71	0.15	0.072	0.018
4#	74.30	0.38	2.97	0.26	0.13	0.040

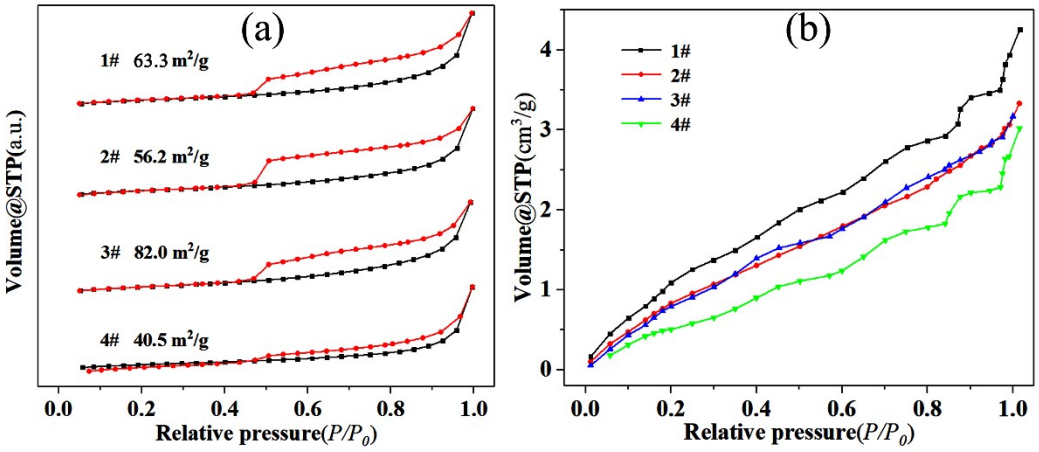

Figure S9. N_2 sorption isotherms (a) and CO_2 sorption isotherms (b) of the Ni-MOFs based on the PET-derived BDC and different leaching solution of the Ni-containing EPS.

Table S2. Surface area and CO_2 adsorption capacity of the Ni-MOF samples

Term/Samp.	**Ni-MOF-C**	**Ni-MOF-W**	**2#**	**3#**	**4#**
$\mathbf{S}_{BET}$ (m^2/g)	49.7	63.3	56.2	82.0	40.5
$\mathbf{Q}_{CO2}$ (cm^3/g)	2.4	3.9	3.3	3.2	3.0

Note: the CO_2 adsorption capacities were recorded at normal temperatures (298K) and pressures (1 atm).

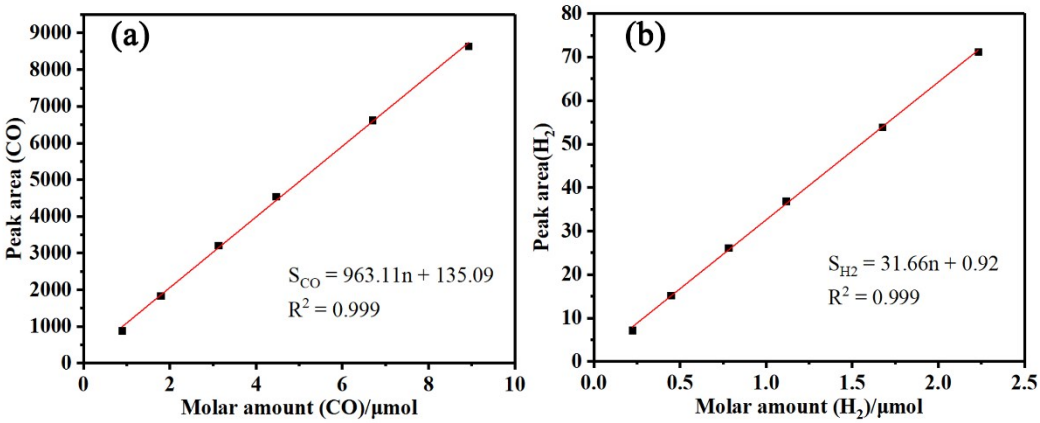

Figure S10. The standard curve of CO (a) and H_2 (b).